RSC Advances

ROYAL SOCIETY OF CHEMISTRY

www.rsc.org/advances

Promotional Effects of Cetyltrimethylammonium Bromide Surface Modification on Hematite Photoanode for Photoelectrochemical Water Splitting

Qian Li,[a,b] Rajini P Antony,[b] Lydia Helena Wong,[b] Dickon H. L. Ng*[a]*

[a] *Department of Physics, The Chinese University of Hong Kong, Hong Kong, China;*

[b] *School of Materials Science and Engineering, Nanyang Technological University, Singapore,639798.*

Prof. Dickon H. L. Ng

*E-mail:dng@phy.cuhk.edu.hk. Tel.: 852 39436392, G8 Science Center North Block, Department of Physics, The Chinese University of Hong Kong, Hong Kong, China

Prof. Lydia Helena Wong

*E-mail: lydiawong@ntu.edu.sg, Tel.: (+65) 6513 8292, N4.1 #02-27a, 50 Nanyang Avenue, School of Materials Science and Engineering, Nanyang Technological University Singapore 639798

Abstract

The hematite nanorod array was treated with cetyltrimethylammonium bromide (CTAB) surfactant by a simple hydrothermal method. The generated CTAB-Fe_2O_3 had doubled the photocurrent of pristine hematite at 1.23 V vs. RHE. We found that there was an increase of carrier density, and the resultant stronger band bending from the CTAB surface modification had favored the transport of the charge carriers. The negative electric field created on the surface of hematite owing to the Br^-layer had sped up the interfacial charge transfer and the oxygen evolution kinetics. Thus, there was an enhancement in water splitting performance. The modification by CTAB on the surface of hematite was proven to be an effective approach in promoting photoelectrochemical water splitting.

Keywords: Hematite, Surface modification, CTAB, Photoelectrochemical water splitting

1. Introduction

It is known that photoelectrochemical (PEC) water splitting can capture and store solar energy in the chemical form [1-5]. Hematite is a promising photoanode candidate for PEC cell due to its low cost, high stability, abundance and suitable band gap (1.9-2.2 eV) [4, 6]. However, its current water splitting efficiency is far below the theoretical value because of the short hole transport distance (2-4nm), slow oxygen evolution reaction (OER) kinetics, unfavourable conduction band position and low photovoltage [4, 7]. To address the above difficulties, the following approaches are being considered: depositing on three dimensional charge collector[8], doping[2, 9], forming heterojunctions[10, 11], loading OER catalyst[7, 12, 13], nanostructuring[14-16] and surface engineering[3, 4, 9, 17, 18].

In some works on surface modification of hematite, Al_2O_3[19], TiO_2[20], ZnO[17] and $Fe_xSn_{1-x}O_4$[4] were coated onto hematite, aiming to passivate surface defects thus promoting the interfacial charge transfer, and cathodically shifting the onset potential. Steier et al.[18] employed Nb_2O_5 and SiO_x as under-layer to improve conductivity and band bending of hematite thereby increasing photocurrent plateau while using Ga_2O_3 as over-layer to passivate surface states thus negatively shifting the onset potential. Moreover, metal oxide surface engineering and ionic species were investigated to modify the surface property of hematite. Hu et al.[9] had modified the Ti-Fe_2O_3 with fluoride which negatively shifted the flat band potential thus achieving the zero bias PEC performance. Kim et al.[3] established a negative electric field on the surface of hematite with phosphate ion (Pi) in order to promote the charge separation and extraction of photoexcited holes to the electrode surface. Qu et al.[21] modified the TiO_2

with Br^- to improve its photodegradation performance. Inspired by these approaches, we had modified the surface of hematite with CTAB for the photoelectrochemical water splitting.

In this communication, we report, for the first time, the synthesis of CTAB modified-Fe_2O_3 nanorods to improve the photoelectrochemical water splitting performance. A simple hydrothermal method was used to modify the hematite to form a stable photoanode. The possible effects of CTAB on hematite was well explored by (photo)electrochemical analysis, and the mechanism involved was proposed. The CTAB surface engineering of hematite had provided a new way for surface treatment of photoanode toward efficient water splitting application.

2. Experiments

2.1 Sample preparation

Fluorine-doped tin oxide (FTO) glass was sequentially cleaned in acetone, ethanol and distilled water. The hematite nanorod array was prepared by hydrothermal method according to the work in previous report [15]. In a typical sample preparation, a 1x1.5 cm^2 FTO was put into autoclave with 12 ml of solution containing 1.5 mmol of $FeCl_3 \cdot 6H_2O$ (from Sigma-Aldrich) and 1.5 mmol of urea (from Sigma-Aldrich) and treated at 100ºC for 10 h. The produced FeOOH was washed by distilled water, dried and further annealed in air at 550ºC for 2 h and at 800ºC for 20 min. As for CTAB engineering of hematite, the as-prepared hematite was placed into 12 ml solution containing 2.5 mg of CTAB, which was then transferred to a 20 mL Teflon-lined autoclave and kept at 100ºC for 6 h. The CTAB-Fe_2O_3 was washed by distilled water and heated at 350 ºC for 4 h before characterization.

2.2 Characterization

X-ray diffraction (XRD) analysis was conducted by a Shimadzu instrument (Lab X, XRD-6000) with Cu K_α radiation (λ=0.1540598 nm). The surface morphology of the samples was examined by a field emission scanning electron microscope (SEM, JSM-7600F). The ultraviolet-visible (UV-Vis) absorption spectra of the samples were obtained by a PerkinElmer Lambda 750S spectrophotometer equipped with an integrated sphere. Fourier transform infrared spectroscopy (FTIR) was conducted on Frontier FT-IR Spectrometer with reflectance mode.

2.3 Photo-electrochemical test

Photo-electrochemical tests were conducted by an electrochemical analyzer (CHI 660D, CH Instruments Inc., Shanghai). In this three-electrode electrochemical cell, the Pt wire, Ag/AgCl and the hematite sample worked as counter electrode, reference electrode and working electrode, respectively. The electrolyte was 1M KOH with a pH level of 13.3. The measured potential vs that of the Ag/AgCl was converted to the reversible hydrogen electrode (RHE) scale according to the Nernst equation ($E_{RHE} = E_{Ag/AgCl} + 0.059pH + 0.197$). A 150 W Xe lamp (Newport 67005) coupled with an air mass (AM) 1.5 filter worked as the simulated light source; and its intensity was calibrated to be 100 mW/cm^2 by a standard silicon solar cell (Newport 91150). The irradiated area was 0.125 cm^2. The incident photon to current efficiency (IPCE) was measured under the same xenon lamp equipped with a monochromator under potential of 1.23 vs RHE. All the photoelectrochemical measurements were done from the front side of FTO glass and repeated for three times. The Mott-Schottky measurements were performed by the same electrochemical analyzer with a supplied

voltage of 5 mV at a frequency of 1 kHz in dark. The electrochemical impedance spectroscopy (EIS) was carried out in the frequency range of 0.1 to 10^5 Hz with an AC voltage amplitude of 5 mV at open circuit potential.

3. Results and discussions

The Fe_2O_3 and CTAB-Fe_2O_3 samples exhibited similar XRD patterns shown in Fig. S1, which could be indexed to the combined phases of α-Fe_2O_3 (JCPDS 33-0664) and SnO_2 (JCPDS 41-1445)[2]. No peaks corresponding to Br related species were observed. The SEM images of Fe_2O_3 and CTAB-Fe_2O_3 samples as shown in Fig. S2, suggested that the hematite nanorod arrays were well formed with this hydrothermal method. The CTAB surface engineering did not change its surface morphology as expected since we used a post and mild method for CTAB modification. So the phase and surface structures of both Fe_2O_3 and CTAB-Fe_2O_3 had clearly indicated that the CTAB engineering had no influence on the hematite phase and morphology. FTIR spectra were collected to analyze the surface property as revealed in Fig.1. The FTIR peaks located 2921, 2853 cm^{-1} over CTAB-Fe_2O_3 could be indexed to asymmetric stretching, symmetric stretching modes of CH_2 in the methylene chains,[21] which confirmed the coupling of CTAB on the surface of hematite.

Fe_2O_3 and CTAB-Fe_2O_3 were subject to the photoelectrochemical cell measurements as shown in Fig. 2. Fig. 2(a) shows the J-V curves of the as-prepared samples under simulated sunlight with an AM1.5 filter. The dark current densities in all cases were negligible. Impressively, the CTAB engineering improved the photocurrent density of pristine hematite from 0.22 mA/cm^2 to 0.44 mA/cm^2 at 1.23 V vs. RHE. The promotional effect of CTAB engineering on hematite could be clearly

observed from the linear J-V curves. To investigate the photoresponse of CTAB-Fe_2O_3, transient photocurrent measurements were carried out during repeated ON/OFF illumination cycles at 1.23 V vs. RHE. As shown in Fig. 2(b), both samples showed prompt and reproducible photocurrent upon each illumination. Moreover, the positive and negative spikes both appeared over Fe_2O_3 and CTAB-Fe_2O_3. The positive spike upon illumination represents the accumulation of holes at the electrode-electrolyte interface without injecting into the electrolyte while the negative spike upon off light represents the recombination of photoinduced electron-hole pairs[15]. The CTAB modified hematite improved the transient photocurrent density of pristine hematite by two folds which indicated a better charge carriers separation and transport of CTAB-Fe_2O_3. To investigate the photoelectrical response, the Incident Photo to Current Efficiency (IPCE) data was collected according to the equation[2] at 1.23 V vs. RHE

$$IPCE(\lambda) = \frac{1240 \times J(\lambda)}{P \times \lambda} \qquad (1)$$

where P and λ are the intensity (mW/cm^2) and the wavelength (nm) of the incident light, respectively; J (λ) is the photocurrent density (mA/cm^2) under the irradiation of single wavelength λ. As shown in Fig. 2(c), the CTAB-Fe_2O_3 exhibited substantial enhanced IPCE value compared with that of the pristine Fe_2O_3 over the range of the measured wavelengths. This result is consistent with the J-V and I-t results. IPCE is defined as a product of $\eta_{absorption}*\eta_{transport}*\eta_{interface}$, where $\eta_{absorption}$: the photo absorption efficiency, $\eta_{transport}$: the efficiency of charge carriers transporting to solid-liquid interface, and $\eta_{interface}$: efficiency of interfacial charge transfer. The photo absorption

of both Fe_2O_3 and CTAB-Fe_2O_3 showed almost the same light absorption profile as shown in Fig. S3, which indicated that CTAB surface engineering did not change the band gap of hematite. As a matter of fact, this is also revealed by their IPCE curves. Both IPCE profiles of Fe_2O_3 and CTAB-Fe_2O_3 drop to about zero at 610 nm, which is in accordance with the band gap of hematite[2]. Thus, the observed enhancement of IPCE should be ascribed to the improved $\eta_{transport}$ or $\eta_{interface}$. To investigate the stability of Fe_2O_3 and CTAB-Fe_2O_3, we had also measured the photocurrent densities of the as-prepared samples at 1.23 V vs. RHE for 1 h under illumination (AM 1.5G, 100 $mWcm^{-2}$). Fig. 2(d) shows that both Fe_2O_3 and CTAB-Fe_2O_3 exhibits stable photocurrent density during the entire investigated time range, indicating the feasibility of CTAB surface engineered hematite for scalable application.

As discussed previously, the PEC enhancement over CTAB-Fe_2O_3 should be attributed to the improved charge transport and interfacial charge transfer. To further confirm this claim, (photo)electrochemical measurements had been carried. The electrochemical impedance spectra were collected under light and the equivalent circuits were illustrated in Fig. 2(e). In bare hematite case, the Rs is resistance of electrolyte and bulk photoanode, R1 represents the charge carrier trapping resistance by surface states and the CPE1 is the bulk photoanode capacitance. R2 is the charge transfer resistance over the interface hematite and electrolyte and CPE2 is corresponding surface state capacitance.[22] Due to CTAB surface modification, we add one more series RC circuit to simulate the impedance spectrum of CTAB-Fe_2O_3. In which (R2, CPE2) illustrates the interface of hematite and Br or CTAB molecular

while (R3, CPE3) illustrates the interface of solid photoanode and electrolyte. The charge transfer resistance over solid to electrolyte interface for Fe_2O_3 and CTAB-Fe_2O_3 were calculated to be 3631, 96 Ω, respectively. This suggests faster charge transfer across the electrode-electrolyte interface, which well supported our previous statements. In the meantime, Rs of Fe_2O_3 and CTAB-Fe_2O_3 were calculated to be 201 and 134 Ω, respectively. The reduced Rs value of CTAB-Fe_2O_3 suggests faster charge transport behavior in the CTAB modified electrode since same electrolyte is used in our system. Moreover, we had calculated the lifetime of the charge carriers based on the bode phase spectra (Fig. 2(f)). There were two peaks on the CTAB-Fe_2O_3 bode profile, corresponding to charge transfer over solid-electrolyte interface (lower frequency) and CTAB molecular-hematite interface (Higher frequency). According to the equation $t=1/(2\pi*f_{peak})^3$, where f_{peak} is lower frequency peak, the electron lifetime of CTAB-Fe_2O_3 and Fe_2O_3 was 0.095s and 0.061s, respectively. This suggests that CTAB engineering has reduced the charge transfer barriers and prolonged the lifetime of generated charge carriers. Besides the charge collection, we had also investigated the surface oxygen evolution kinetics. Fig. 2(g) displays the Tafel plots of CTAB-Fe_2O_3 and Fe_2O_3 under dark condition. The smaller slope of CTAB-Fe_2O_3 (141mV/decade) compared with that of Fe_2O_3 (192mV/decade) indicates the faster oxygen evolution reaction (OER) kinetics. There is a possibility that the trace adsorbed Br from CTAB could worked as electrocatalyst as suggested by previous report[21]. So far, the impedance spectra and Tafel measurements demonstrate that the CTAB surface engineering contributes to the $\eta_{interface}$ thus

promoting the overall PEC performance. Mott-Schottky curves were collected to explore the carrier density and flat band potential as shown in Fig. 2(h). The calculations were based on the Mott-Schottky equation[2]

$$\left(\frac{A}{C}\right)^2 = \frac{2}{\epsilon_0 \varepsilon \varepsilon_0 N_d}\left(E - E_{fb} - \frac{kT}{q}\right) \quad (2)$$

where A is the surface area of the electrode, C is the capacitance of the space charge layer, N_d is the donor density, E_{fb} is the flat band potential, e_0 is the electronic charge (1.602×10^{-19}C), ε is the dielectric constant of the semiconductor (32) and ε_0 is the permittivity in vacuum (8.854×10^{-14} F/cm^{-1}). The carrier density of CTAB-Fe_2O_3 and Fe_2O_3 are determined to be $0.87*10^{18}$ and $0.45*10^{18}$ cm^{-3}, respectively, which suggests that the CTAB engineering improves the surface carrier density thus favoring the charge transport ($\eta_{transport}$). In view of the above analysis, it is reasonable to conclude that the surface modification by CTAB engineering has improved the efficiency of charge transport ($\eta_{transport}$) and charge transfer ($\eta_{interface}$) simultaneously thereby improving the overall photoelectrochemical water splitting. Based on the electrochemical analysis, we propose the possible promotional mechanism of CTAB surface engineering on hematite as displayed in Fig. 3. When the hematite is treated with CTAB in hydrothermal condition, the Br^- is attached to the surface of hematite by hydrogen bond[21]. So a negative electric field was established on the surface of electrode, which would extract the photoinduced holes[3]. Thereafter, Br^- transformed into the active Br which oxidized the H_2O to O_2 and simultaneously it is reduced back to Br^-. Compared with the pristine hematite, the CTAB-Fe_2O_3 exhibits more efficient charge collection and OER kinetics thus presenting better PEC efficiency.

4. Conclusions

CTAB surface engineering of hematite is carried out by a simple hydrothermal method. The CTAB engineering promotes the charge transport and surface charge reaction thus improving the overall photoelectrochemical water splitting significantly. This method could be applied to improve other photoanode toward efficient photoelectrochemical cell.

Acknowledgements

This work was supported by the Hong Kong SAR Government RGC Earmarked Research Grant 2014/15 (Ref. No. 415206; Project code: 2150491); and a Direct Grant for Research (Project code: 4053076; 2013/14) from the Faculty of Science, The Chinese University of Hong Kong.

References

1. A. C. Nielander, M. R. Shaner, K. M. Papadantonakis, S. A. Francis and N. S. Lewis, *Energy Environ. Sci.* , 2015, 8, 16-25.
2. Y. Ling, G. Wang, D. Wheeler, J. Zhang and Y. Li, *Nano Lett.* , 2011, 11, 2119-2125.
3. J. Y. Kim, J.-W. Jang, D. H. Youn, G. Magesh and J. S. Lee, *Adv. Energy Mater.*, 2014, 4, 1400476-1400483.
4. L. Xi, S. Y. Chiam, W. F. Mak, P. D. Tran, J. Barber, S. C. J. Loo and L. H. Wong, *Chemical Science*, 2013, 4, 164-169.
5. P. S. Bassi, Gurudayal, L. H. Wong and J. Barber, *Phys. Chem. Chem. Phys.* , 2014, 16, 11834-11842.
6. K. Sivula, F. Le Formal and M. Grätzel, *ChemSusChem*, 2011, 4, 432-449.
7. Q. Li, J. Bian, N. Zhang and D. H. L. Ng, *Electrochim. Acta* 2015, 155, 383-390.
8. Y. Qiu, S.-F. Leung, Q. Zhang, B. Hua, Q. Lin, Z. Wei, K.-H. Tsui, Y. Zhang, S. Yang and Z. Fan, *Nano Lett.* , 2014, 14, 2123-2129.
9. Y.-S. Hu, A. Kleiman-Shwarsctein, G. D. Stucky and E. W. McFarland, *Chem. Commun.* , 2009, 2652-2654.
10. Y. Hou, F. Zuo, A. Dagg and P. Feng, *Angew. Chem.*, 2013, 125, 1286-1290.
11. C. Du, X. Yang, M. T. Mayer, H. Hoyt, J. Xie, G. McMahon, G. Bischoping and D. Wang, *Angew. Chem. Int. Ed.* , 2013, 52, 12692 –12695.
12. D. K. Zhong, M. Cornuz, K. Sivula, M. Gratzel and D. R. Gamelin, *Energy Environ. Sci.* , 2011, 4, 1759-1764.

13. L. Xi, P. D. Tran, S. Y. Chiam, P. S. Bassi, W. F. Mak, H. K. Mulmudi, S. K. Batabyal, J. Barber, J. S. C. Loo and L. H. Wong, *J. Phys. Chem. C*, 2012, 116, 13884-13889.

14. D. A. Wheeler, G. Wang, Y. Ling, Y. Li and J. Z. Zhang, *Energy Environ. Sci.* , 2012, 5, 6682-6702.

15. Gurudayal, S. Y. Chiam, M. H. Kumar, P. S. Bassi, H. L. Seng, J. Barber and L. H. Wong, *ACS Appl. Mat. Interfaces*, 2014, 6, 5852-5859.

16. S. C. Warren, K. Voïtchovsky, H. Dotan, C. M. Leroy, M. Cornuz, F. Stellacci, C. Hébert, A. Rothschild and M. Grätzel, *Nat. Mater.* , 2013, 12, 842-849.

17. L. Xi, P. S. Bassi, S. Y. Chiam, W. F. Mak, P. D. Tran, J. Barber, J. S. Chye Loo and L. H. Wong, *Nanoscale*, 2012, 4, 4430-4433.

18. L. Steier, I. Herraiz-Cardona, S. Gimenez, F. Fabregat-Santiago, J. Bisquert, S. D. Tilley and M. Grätzel, *Adv. Funct. Mater.* , 2014, 24, 7681–7688.

19. Z. Fu, T. Jiang, L. Zhang, B. Liu, D. Wang, L. Wang and T. Xie, *J. Mater. Chem. A*, 2014, 2, 13705-13712.

20. X. Yang, R. Liu, C. Du, P. Dai, Z. Zheng and D. Wang, *ACS Appl. Mat. Interfaces*, 2014, *6* (15), 12005–12011.

21. Y. Qu, W. Wang, L. Jing, S. Song, X. Shi, L. Xue and H. Fu, *Appl. Surf. Sci.* , 2010, 257, 151-156.

22. B. Klahr, S. Gimenez, F. Fabregat-Santiago, T. Hamann and J. Bisquert, *J. Am. Chem. Soc.* , 2012, 134, 4294-4302.

Figure and figure captions

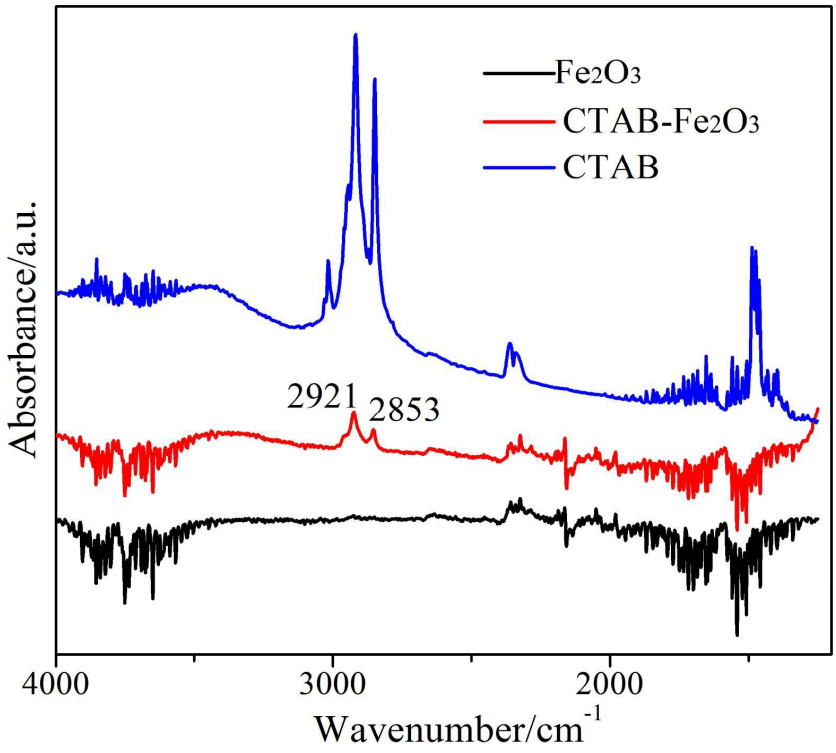

Fig.1 FTIR spectra of Fe_2O_3, CTAB-Fe_2O_3 and CTAB.

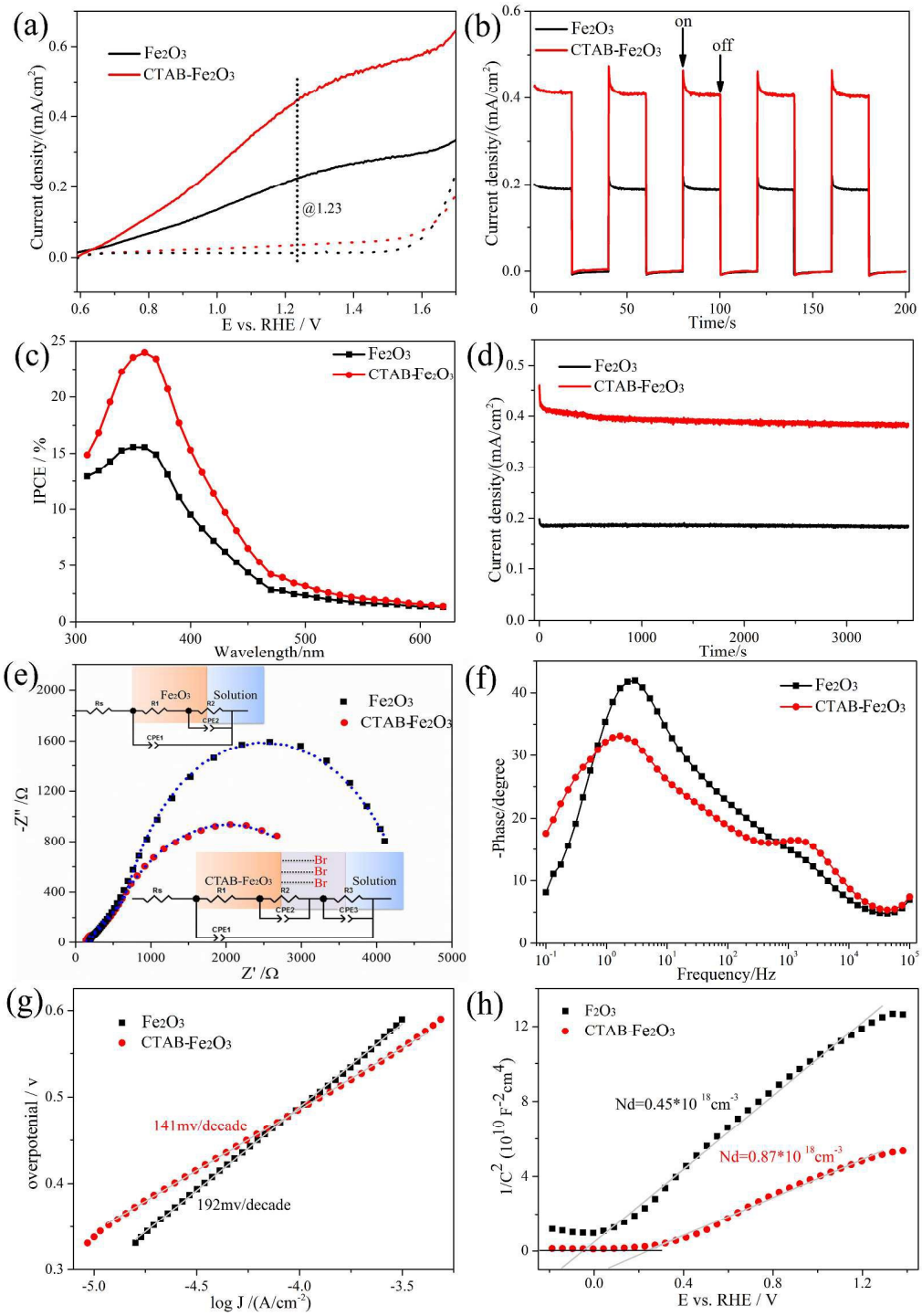

Fig. 2 (a) J-V curves under simulated sunlight with AM1.5 filter; (b) Transient I-t curves, (c) IPCE measurements, (d) Long time I-t curves of Fe_2O_3 and CTAB-Fe_2O_3 at 1.23 V vs. RHE, (e) Nyquist plots, (f) Bode phase plots, (g) Tafel plots (h) Mott-Schottky plots of Fe_2O_3 and CTAB-Fe_2O_3.

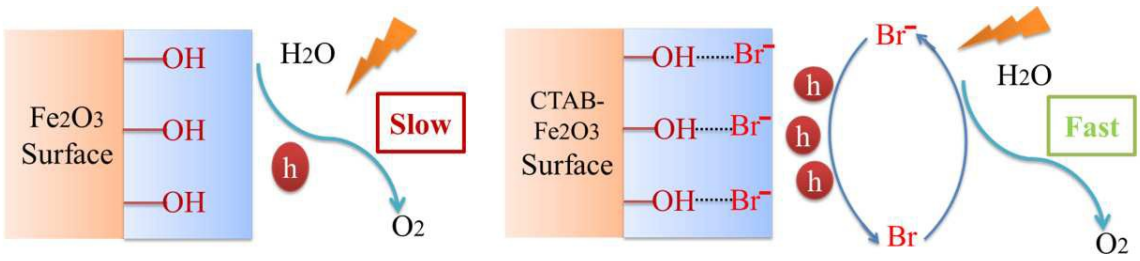

Fig. 3 The promotional mechanism of CTAB surface engineering on hematite.